

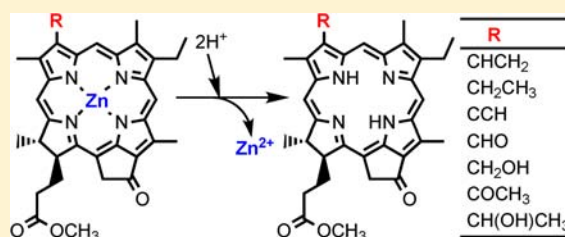
Systematic Analysis of the Demetalation Kinetics of Zinc Chlorophyll Derivatives Possessing Different Substituents at the 3-Position: Effects of the Electron-Withdrawing and Electron-Donating Strength of Peripheral Substituents

Yoshitaka Saga,* Yuta Kobashiri, and Kana Sadaoka

Department of Chemistry, Faculty of Science and Engineering, Kinki University, Higashi-Osaka, Osaka 577-8502, Japan

Supporting Information

ABSTRACT: Removal of the central metal from chlorophyll (Chl) molecules is biologically important in terms of production of the primary electron acceptors in photosystem-II photosynthetic reaction centers and the early stage in Chl degradation. The physicochemical properties on demetalation of chlorophyllous pigments are useful in the understanding of such reaction mechanisms in photosynthetic organisms. Here we analyzed the demetalation kinetics of a series of Zn-Chl derivatives with a systematic variation in the electron-withdrawing and -donating substituents at the 3-position of the chlorin macrocycle under acidic conditions to elucidate thoroughly the substitution effects on the demetalation properties of chlorophyllous pigments. Dehydrogenation of the aliphatic group ($\text{CH}_2\text{CH}_3 \rightarrow \text{CH}=\text{CH}_2 \rightarrow \text{C}\equiv\text{CH}$) at the 3-position slowed the removal of the central zinc from the chlorin macrocycle. The gradual decrease in the demetalation rate constants of the three zinc chlorins originates from differences in the electron-withdrawing strength of the ethyl, vinyl, and ethynyl groups directly linked to the chlorin π macrocycle. Reduction of the 3¹-carbonyl groups significantly increased the demetalation rate constants, and the relative ratios of the demetalation rate constants of the zinc chlorins possessing a carbonyl group to those possessing the corresponding hydroxy group were analogous in the cases of 3-formyl- and 3-acetyl-zinc chlorins. The demetalation rate constants of the seven Zn-Chl derivatives possessing various electron-withdrawing and -donating groups exhibited good correlation with the Hammett σ parameters of the 3-position substituents.



INTRODUCTION

Chlorophyll (Chl) and bacteriochlorophyll (BChl) molecules play important roles in photosynthesis, which is an efficient sunlight conversion system in nature.^{1,2} These chlorophyllous pigments have tetrapyrrole macrocycles as the photofunctional moieties and commonly possess a central magnesium in the π macrocycle. The exceptions in photosynthetically active pigments are Zn-BChl *a* in a purple bacterium *Acidiphilium rubrum*^{3–5} and demetalated pigments of (B)Chl molecules in photosystem (PS)-II-type photosynthetic reaction centers.^{6–11}

PS-II reaction centers in oxygenic photosynthetic organisms utilize pheophytin (Phe) *a*, which lacks the central magnesium from Chl *a*, as the primary electron acceptor.^{6–9} In PS-II, cofactors are positioned with pseudo-2-fold symmetry.^{9,12–15} Therefore, two Phe *a* molecules are present in the protein scaffolds of PS-II, but only one Phe *a* participates in photoinduced electron transfer. Biosynthesis of Phe *a* in PS-II is completely unknown in spite of its biological importance. Phe *a* would be produced from Chl *a* by its demetalation because Chl synthase uses Chlide *a* as a substrate to esterify a long hydrocarbon chain at the 17-propionate and cannot use pheophorbide *a* lacking the central magnesium.¹⁶ From this viewpoint, Chl demetalation is crucial for the in vivo production of Phe molecules, which function as the primary

electron acceptors in PS-II-type photosynthetic reaction centers.

Another important event concerning demetalation of chlorophyllous pigments is found in the Chl degradation pathway. Chl degradation is one of the most large-scale bioprocesses on earth and a major origin of beautiful phenomena in autumn.^{17–21} Removal of the central magnesium from the chlorin macrocycle occurs in the early stage of the degradation process, but its mechanism has not been thoroughly unraveled yet.

In vitro demetalation of natural Chl molecules and their model compounds has been examined^{21–37} because the physicochemical properties of Chl demetalation are clues to understanding such biologically important reactions in photosynthetic organisms. Some of the previous studies on in vitro Chl demetalation demonstrated that peripheral substituents on the chlorin macrocycle had large effects on the demetalation properties of chlorophyllous pigments.^{22,23,28,30–32,34–37} For example, a comparison of the demetalation kinetics between Chl *a* and *b* indicated that the 7-formyl group in Chl *b* was responsible for significantly slow demetalation kinetics.^{22,23,28,32}

Received: July 31, 2012

Published: December 11, 2012

We reported that formyl groups in other naturally occurring pigments such as Chl *d* and BChl *e* also made their demetalation kinetics slow.^{30–32} The effects of the formyl groups in these pigments on the demetalation properties are ascribable to their electron-withdrawing abilities. However, no quantitative information is available on the relationship between the electron-withdrawing/-donating strength of the peripheral substituents and demetalation kinetics of chlorophyllous pigments. We report herein the demetalation properties of synthesized zinc chlorins 1–7, in which only 3-position substituents are different from each other. Figure 1

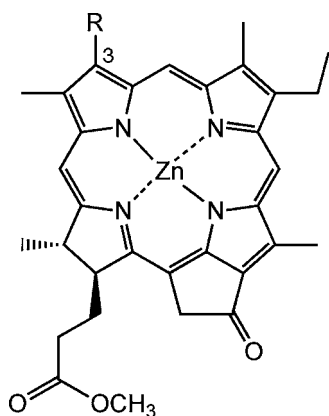


Figure 1. Molecular structures of zinc chlorins 1–7 used in the present study: 1, R = CH=CH₂; 2, R = CH₂CH₃; 3, R = C≡CH; 4, R = CHO; 5, R = CH₂OH; 6, R = COCH₃; 7, R = CH(OH)CH₃.

shows the molecular structures of zinc chlorins 1–7 used in this study. Zinc chlorin 1 has a vinyl group at the 3-position and is a good model compound of Chl *a*. The vinyl group is hydrogenated (3-CH=CH₂ → 3-CH₂CH₃) and dehydrogenated (3-CH=CH₂ → 3-C≡CH) in zinc chlorins 2 and 3, respectively. Zinc chlorin 4 possessing a formyl group at the 3-position is a derivative of Chl *d*, which is a unique photosynthetic pigment in *Acaryochloris marina*.^{38,39} An acetyl group in zinc chlorin 6 is a peripheral substituent characteristic of BChl *a* and *b* in anoxygenic photosynthetic bacteria.^{1,2} Reduction of the 3¹-carbonyl groups in 4 and 6 affords zinc chlorins 5 and 7, respectively. Zinc chlorins 5 and 7 possessing a 3¹-hydroxy group have widely been used as model compounds of light-harvesting BChl *c* and *d* in green photosynthetic bacteria.^{40–44} A comparison of the demetalation properties among 1–7 enables us to understand the inductive effects of the 3-position substituents on the demetalation properties of metallochlorins quantitatively without other substitution effects.

EXPERIMENTAL SECTION

Apparatus. Visible absorption spectra were measured with a Shimadzu UV-2450 spectrophotometer, where the reaction temperature was regulated with a Shimadzu thermoelectric temperature-controlled cell holder TCC-240A. High-performance liquid chromatography (HPLC) was performed with a Shimadzu LC-20AT pump and an SPD-M20A or SPD-20AV detector. Mass spectrometry (MS) spectra were measured with a JEOL JMS700 spectrometer; *m*-nitrobenzyl alcohol was used as a matrix.

Materials. Zinc chlorins 1–7 were synthesized from Chl *a*, which was extracted from cyanobacterium *Spirulina geitleri*, according to previous reports.^{2,45–54} Methyl pyropheophorbide *a* (1') was synthesized from Chl *a* through three steps.^{45,46} The 3-vinyl group

of 1' was hydrogenated in the presence of palladium charcoal under a hydrogen atmosphere to give methyl 3-devinyl-3-ethyl-pyropheophorbide *a* (2').⁴⁵ The 3-vinyl group in 1' was oxidatively cleaved by sodium periodate and osmium tetroxide to give methyl 3-devinyl-3-formyl-pyropheophorbide *a* (4').^{46,47} Subsequent reduction of the 3-formyl group in 4' by *tert*-butylamine borane complexes afforded methyl 3-devinyl-3-hydroxymethyl-pyropheophorbide *a* (5').^{46,48} The formyl group in 4' was converted to the ethynyl group to give methyl 3-devinyl-3-ethynyl-pyropheophorbide *a* (3') by treatment with a commercially available Bestmann–Ohira reagent [(MeO)₂P(O)C(COMe)N₂] in the presence of Cs₂CO₃.^{49,50} The 3-vinyl group in 1' was converted to the hydroxyethyl group using hydrogen bromide,^{51,52} followed by the formation of methyl ester by treatment with (trimethylsilyl)diazomethane⁵³ to give methyl 3-devinyl-3-hydroxyethyl-pyropheophorbide *a* (7'). The hydroxyethyl group in 7' was oxidized to produce methyl 3-devinyl-3-acetyl-pyropheophorbide *a* (6') possessing the 3-acetyl group by use of 4-methylmorpholine-*N*-oxide and tetrapropylammonium perruthenate.⁵⁴ Zinc was inserted into free-base chlorins 1'–7' by Zn(CH₃COO)·2H₂O to afford zinc chlorins 1–7, respectively. The synthesized zinc chlorins were purified by reverse-phase HPLC before measurements of the demetalation kinetics.

Characteristic spectral data of 1–7 are described as follows (see also refs 45–54). Zinc methyl pyropheophorbide *a* (1). UV–vis (acetone): λ_{max} = 655 nm (relative intensity 0.69), 607 (0.11), 568 (0.06), 524 (0.04), 425 (1.00), 405 (0.60). MS (FAB). Calcd for C₃₄H₃₄N₄O₃Zn (M⁺): *m/z* 610.19. Found: *m/z* 610.26. Zinc methyl 3-devinyl-3-ethylpyropheophorbide *a* (2). UV–vis (acetone): λ_{max} = 643 nm (relative intensity 0.77), 598 (0.12), 562 (0.06), 518 (0.03), 421 (1.00), 401 (0.65). MS (FAB). Calcd for C₃₄H₃₆N₄O₃Zn (M⁺): *m/z* 612.21. Found: *m/z* 612.28. Zinc methyl 3-devinyl-3-ethynyl-pyropheophorbide *a* (3). UV–vis (acetone): λ_{max} = 661 nm (relative intensity 0.76), 613 (0.10), 571 (0.05), 527 (0.03), 428 (1.00), 408 (0.52). MS (FAB). Calcd for C₃₄H₃₂N₄O₃Zn (M⁺): *m/z* 608.18. Found: *m/z* 608.22. Zinc methyl 3-devinyl-3-formyl-pyropheophorbide *a* (4). UV–vis (acetone): λ_{max} = 680 nm (relative intensity 0.95), 631 (0.12), 586 (0.08), 541 (0.04), 443 (1.00). MS (FAB). Calcd for C₃₃H₃₂N₄O₄Zn (M⁺): *m/z* 612.17. Found: *m/z* 612.25. Zinc methyl 3-devinyl-3-hydroxymethyl-pyropheophorbide *a* (5). UV–vis (acetone): λ_{max} = 646 nm (relative intensity 0.76), 601 (0.12), 565 (0.06), 519 (0.04), 423 (1.00), 403 (0.64). MS (FAB). Calcd for C₃₃H₃₄N₄O₄Zn (M⁺): *m/z* 614.19. Found: *m/z* 614.24. Zinc methyl 3-devinyl-3-acetyl-pyropheophorbide *a* (6). UV–vis (acetone): λ_{max} = 668 nm (relative intensity 0.73), 619 (0.13), 579 (0.08), 533 (0.04), 432 (1.00). MS (FAB). Calcd for C₃₄H₃₄N₄O₄Zn (M⁺): *m/z* 626.19. Found: *m/z* 626.23. Zinc methyl 3-devinyl-3-hydroxyethyl-pyropheophorbide *a* (7). UV–vis (acetone): λ_{max} = 645 nm (relative intensity 0.78), 600 (0.12), 565 (0.06), 519 (0.03), 422 (1.00), 402 (0.65). MS (FAB). Calcd for C₃₄H₃₆N₄O₄Zn (M⁺): *m/z* 628.20. Found: *m/z* 628.30.

Measurements of the Demetalation Kinetics. A 3.0 mL acetone solution of purified zinc chlorins (Soret absorbance = 1.0) was mixed with 975 μL of distilled water. Then, 25 μL of aqueous hydrochloric acid for volumetric analysis (Wako Pure Chemical Industries, Ltd., Japan) was added to the solutions, and absorbance at the Soret peak positions of zinc chlorins was measured under the control of reaction temperatures at 25 °C.

Pigment Analysis after Demetalation. After demetalation reactions, the solutions were neutralized by 4% aqueous NaHCO₃. The reaction products were extracted with dichloromethane, washed with NaCl-saturated water, and dried over anhydrous Na₂SO₄. The solutions were filtered and dried with nitrogen gas. The residues were analyzed by reverse-phase HPLC.

RESULTS AND DISCUSSION

Spectral Changes. Demetalation of synthetic zinc chlorins 1–7 possessing a different substituent at the 3-position was kinetically analyzed in acidic aqueous acetone. Figure 2 depicts a spectral change of zinc chlorin 1 possessing the 3-vinyl group

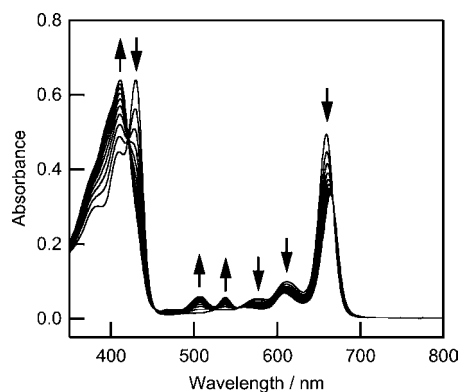


Figure 2. Spectral change of zinc chlorin **1** in acetone/water [3:1 (v/v)] at the proton concentration of 6.3×10^{-3} M. Spectra from 0 to 540 min at a 60-min interval. The arrows show the direction of the absorbance changes.

during the demetalation process at the proton concentration of 6.3×10^{-3} M. Zinc chlorin **1** exhibited the Soret and Q_y bands at 430 and 659 nm before demetalation in this solution [acetone:water = 3:1 (v/v)]. The Soret absorption band of **1** gradually decreased with an appearance of a new absorption band at 411 nm under this condition. This 411-nm absorption band was ascribable to the Soret band of the demetalation form of **1**, namely, **1'**. The Q_y absorbance of **1** at 659 nm decreased simultaneously under acidic conditions. The small absorption bands at 577 and 612 nm of **1** also became small gradually, and the absorption bands at 507 and 537 nm, which was ascribable to **1'**, appeared. The isosbestic points were present at 421, 453, 554, and 667 nm in this spectral change.

Essentially the same spectral changes were observed in demetalation reactions of **2**–**7** in acidic aqueous acetone (data not shown). The Soret and Q_y absorption bands of zinc chlorins **2**–**7** decreased and new Soret bands of the corresponding free-base forms (**2'**–**7'**, respectively) appeared at the shorter-wavelength side of the Soret band of zinc chlorins with several isosbestic points. The differences of the Soret peak positions between zinc chlorins **1**–**7** and the corresponding free-base chlorins **1'**–**7'** were 15–24 nm (900 – 1300 cm^{-1}). This allows us to analyze their demetalation reactions kinetically by monitoring the absorbance changes at the Soret peak positions of **1**–**7**.

Demetalation Kinetics. Figure 3 depicts time courses of Soret absorbance of zinc chlorins **1**–**7** through demetalation at the proton concentration of 3.8×10^{-2} M. All of the kinetic plots exhibited linear relationships between the logarithm of the Soret absorbance and reaction time. The demetalation reactions of zinc chlorins **1**–**7**, therefore, can be regarded as pseudo-first-order. Such pseudo-first-order kinetics was also observed in demetalation reactions of **1**–**7** at the lower proton concentrations between 3.1×10^{-2} and 6.3×10^{-3} M. These are in line with the reaction conditions in which the proton concentration was much higher than the concentration of zinc chlorins. Demetalation rate constants, k 's, were determined by fitting the time courses of Soret absorbances of zinc chlorins **1**–**7** to the following kinetic equation:

$$\ln(A - A_\infty)/(A_0 - A_\infty) = -kt$$

where A_0 , A , and A_∞ are Soret absorbances of zinc chlorins at the onset of the measurement, at time t , and at complete demetalation, respectively. The demetalation rate constants of

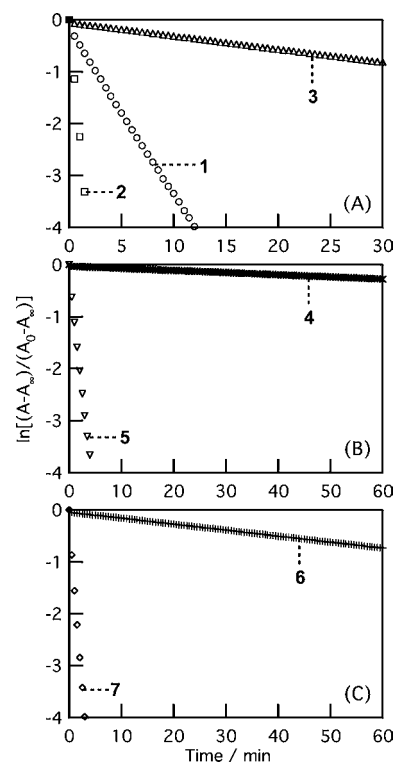


Figure 3. Demetalation kinetics of **1**–**3** (A), **4** and **5** (B), and **6** and **7** (C) in acetone/water [3:1 (v/v)] at the proton concentration of 3.8×10^{-2} M. Absorbance changes were monitored at 430, 424, 433, 450, 427, 438, and 426 nm for **1**–**7**, respectively. A_0 , A , and A_∞ are Soret absorbances of zinc chlorins at the onset of measurements, at time t , and at complete demetalation, respectively.

1–**7**, which were the averages of three independent measurements, were plotted in Figure 4 against the logarithm of the

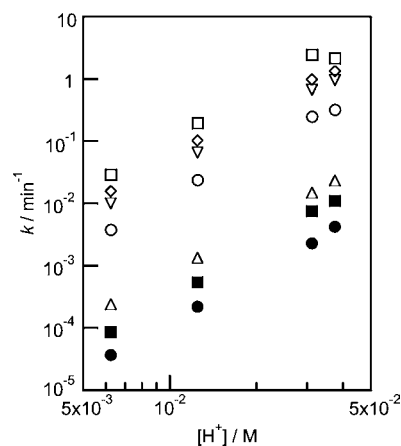


Figure 4. Demetalation rate constants of **1** (open circles), **2** (open squares), **3** (open triangles), **4** (closed circles), **5** (open reverse triangles), **6** (closed squares), and **7** (open diamonds) in acetone/water [3:1 (v/v)] depending on the examined proton concentrations.

proton concentrations, $\log [H^+]$. The logarithm of the demetalation rate constants, $\log k$, of **1**–**7** increased linearly with $\log [H^+]$. The slopes of $\log k$ of **1**–**7** against $\log [H^+]$ in Figure 4 were estimated to be 2.5, 2.6, 2.6, 2.6, 2.6, 2.8, and 2.5, respectively. These values were slightly larger than those of natural and seminatural Chl molecules (magnesium chlorins) reported previously: the slopes of these Chl molecules in the

log k versus log $[H^+]$ plots were estimated to be ca. 2 at proton concentrations of around 10^{-3} M.^{27–29,37} One possible reason for the differences of the slopes between zinc chlorins in this study and (semi)natural Chl molecules in the previous reports would be the effects of the central metals. Kobayashi et al. reported that the slopes of zinc complexes (1.94 and 2.17 for Zn-Chl *a* and Zn-BChl *a*, respectively) were larger than those of the corresponding magnesium complexes (1.70 and 1.74 for Mg-Chl *a* and Mg-BChl *a*, respectively).²⁹ Therefore, slightly larger values of the slopes in the plots of the demetalation rate constants against the proton concentrations for zinc chlorins 1–7 are in line with the tendency in the previous work, although further studies will be required for understanding the origin of such differences.

Effects of the Aliphatic Groups on the Demetalation Kinetics. Zinc chlorins 1–3 possess vinyl, ethyl, and ethynyl groups, respectively, at the 3-position. Therefore, a comparison of the demetalation rate constants among 1–3 allows us to investigate the effects of the aliphatic groups on the demetalation properties of chlorophyllous pigments systematically. The order of the demetalation rate constants is $2 > 1 > 3$ under acidic conditions, as shown in Figures 3A and 4. The relative ratio of the demetalation rate constants of 3 to those of 1, $k(3)/k(1)$, were distributed from 5.5×10^{-2} to 7.3×10^{-2} at the proton concentration range between 3.8×10^{-2} and 6.3×10^{-3} M. These values were slightly smaller than the relative ratio of $k(1)/k(2)$, which were estimated within 1.0×10^{-1} and 1.5×10^{-1} , under the corresponding conditions.

The effects of dehydrogenation of the 3-aliphatic groups on the demetalation kinetics can be rationalized by invoking differences of the electron-withdrawing abilities among the three groups. Figure 5 depicts the relationship between the

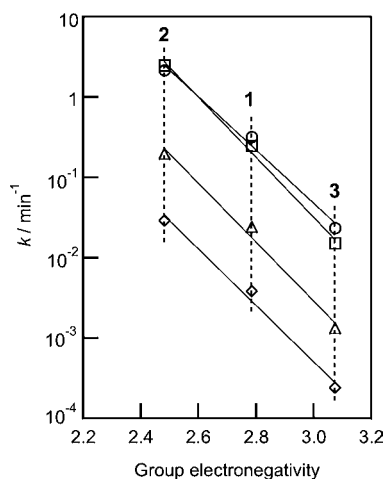


Figure 5. Dependence of the demetalation rate constants of zinc chlorins 1–3 at the proton concentrations of 3.8×10^{-2} (open circles), 3.1×10^{-2} (open squares), 1.3×10^{-2} (open triangles), and 6.3×10^{-3} M (open diamonds) on the group electronegativities⁴⁵ of the substituents.

demetalation rate constants of 1–3 and the group electronegativities of the 3-position substituents in 1–3 estimated by Inamoto and Masuda.⁵⁵ Good correlations between their demetalation rate constants and the group electronegativities were observed under these conditions: the correlation coefficients $|r|$ were estimated to be 0.995, 0.998, 0.994, and 0.995 at the proton concentrations of 3.8×10^{-2} , 3.1×10^{-2} ,

1.3×10^{-2} , and 6.3×10^{-3} M, respectively. The demetalation rate constants of 1–3 were also correlated with the Hammett σ parameters of these groups,⁵⁶ as described below. It was reported that electron-withdrawing formyl and acetyl substituents on the chlorin π macrocycle slowed removal of the central metal because such substituents decreased the electron densities of the core nitrogen atoms and suppressed an electrophilic attack of protons to the nitrogen atoms.^{31,32,34,35} This kinetic analysis clearly indicates that the electron-withdrawing abilities of the aliphatic groups connected to the chlorin macrocycle were also responsible for the demetalation properties of Chl derivatives.

Effects of Reduction of the Carbonyl Groups on the Demetalation Kinetics. The present study revealed that reduction of the formyl and acetyl groups at the 3-position of the chlorin macrocycle accelerated their demetalation kinetics. The relative ratios of the demetalation rate constants of 4 possessing the 3-formyl group to those of 5 possessing the 3-hydroxymethyl group were distributed from 3.4×10^{-3} to 4.3×10^{-3} in the proton concentration range between 3.8×10^{-2} and 6.3×10^{-3} M and were similar to the cases of 6 possessing the 3-acetyl group and 7 possessing the 3-hydroxyethyl group [the relative ratios of $k(6)/k(7)$ ranged between 5.2×10^{-3} and 8.3×10^{-3} under the same conditions]. These suggest that the 3-acetyl group affected the demetalation properties of metallochlorins in a manner similar to that of the 3-formyl group. We previously compared the demetalation kinetics between 7-formyl- and 7-hydroxymethyl-metallochlorins: the relative ratio of the demetalation rate constant of the 7-formyl-zinc chlorin to that of the 7-hydroxymethyl-zinc chlorin was 5.3×10^{-3} at the proton concentration of 3.8×10^{-2} M.³⁴ This value is analogous to the relative ratio of 4 to that of 5 under the same conditions [$k(4)/k(5) = 4.3 \times 10^{-3}$], suggesting that reduction of the formyl group in the B-ring of the chlorin macrocycle had almost the same effects on the demetalation properties as that in the A-ring.

Correlation between the Demetalation Rate Constants and Hammett σ Parameters. Hammett σ constants are some of the most important parameters for interpretation of organic reactions and have successfully been applied to elucidation of various reaction mechanisms.⁵⁶ The demetalation rate constants of zinc chlorins 1–7 were plotted against Hammett σ_m and σ_p parameters of the 3-position substituents in Figures 6 and 7, respectively. The k values of 1–7 exhibited high correlation coefficients $|r|$ of 0.951–0.956 and 0.953–0.964 with the Hammett σ_m and σ_p constants, respectively, under acidic conditions. The correlation coefficients with σ_m were quite similar to those with σ_p . These indicate that the kinetic stabilities for removal of the central metal from chlorophyllous pigments could be quantitatively rationalized by invoking the electron-withdrawing and -donating strength of the substituents directly linked to the chlorin π macrocycle. The good correlation in the present study is in agreement with the previous results of the oxidation potentials⁵⁷ and monoprotation equilibrium constants⁵⁸ of β -substituted porphyrins, in which these physicochemical properties were correlated with the Hammett σ parameters of the β substituents.

Recently, the metalation and demetalation properties of chlorophyllous pigments have been reported.^{59–62} Several factors such as the macrocyclic structures, peripheral substituents, and axial coordination were assumed to be responsible for these properties. Orzel et al. reported that the peripheral carbonyl groups suppressed the reactivity of

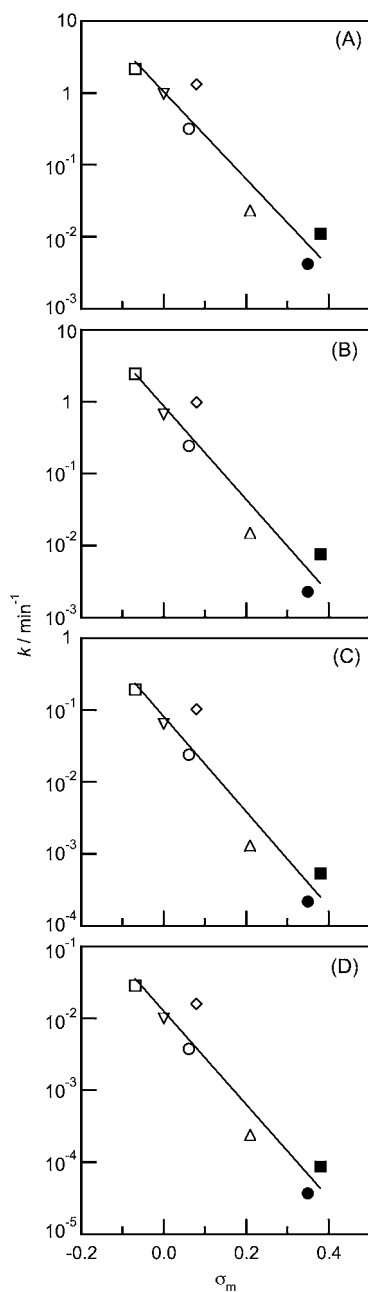


Figure 6. Dependence of the demetalation rate constants of zinc chlorins 1–7 at the proton concentrations of 3.8×10^{-2} (A), 3.1×10^{-2} (B), 1.3×10^{-2} (C), and 6.3×10^{-3} M (D) on the Hammett σ_m constants⁴⁶ of substitution groups: 1 (open circles), 2 (open squares), 3 (open triangles), 4 (closed circles), 5 (open reverse-triangles), 6 (closed squares), and 7 (open diamonds).

metalation.⁶⁰ Such effects would be consistent with the present results. It is noted that the possibility of protonation at the 13¹-carbonyl group in the isocyclic E-ring was ruled out under the present reaction conditions, judged from the temporal changes of visible absorption spectra through demetalation and HPLC analyses of the reaction products (Figure 8). This is in line with the lack of the 13²-methoxycarbonyl group in zinc chlorins 1–7.

HPLC Analysis of the Reaction Products. Figure 8 shows HPLC elution patterns of the reaction products of 1–7 in acetone/water (3:1) at the proton concentration of 3.8×10^{-2} M. After the demetalation reaction of 1, the main fraction was

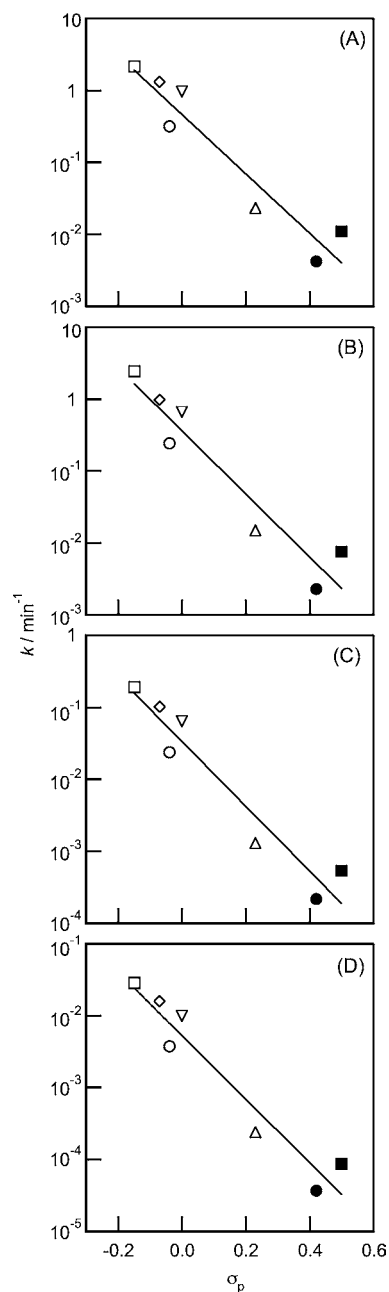


Figure 7. Dependence of the demetalation rate constants of zinc chlorins 1–7 at the proton concentrations of 3.8×10^{-2} (A), 3.1×10^{-2} (B), 1.3×10^{-2} (C), and 6.3×10^{-3} M (D) on the Hammett σ_p constants⁴⁶ of substitution groups: 1 (open circles), 2 (open squares), 3 (open triangles), 4 (closed circles), 5 (open reverse-triangles), 6 (closed squares), and 7 (open diamonds).

observed at 42 min (Figure 8A). This fraction exhibited Soret and Q_y bands at 407 and 665 nm, respectively, in the HPLC eluent, and was ascribed to the free-base form of 1, namely, 1'. No other fractions were detected, indicating no side reactions under the present conditions. HPLC analysis of the reaction products of 2–7 gave similar results. In the HPLC chromatogram of the reaction products of 2, the sole fraction, which had Soret and Q_y bands at 404 and 654 nm, respectively, was detected at 44 min (Figure 8B). This fraction could be assigned to 2'. The reaction products of 3 gave the main fraction of 3' at 30 min ($\lambda_{\max} = 407$ and 673 nm) with a slight byproduct at 13 min (Figure 8C). The chromatograms of reaction products of 4

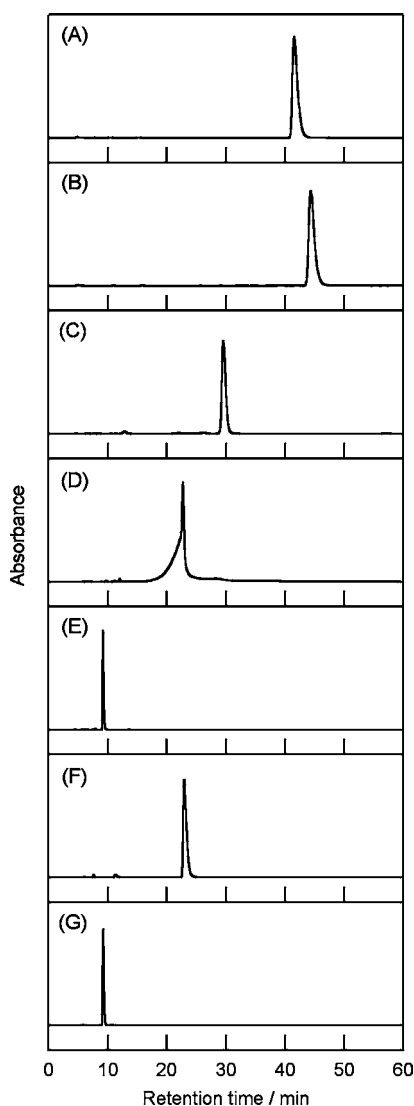


Figure 8. HPLC elution patterns of the reaction products of **1** (A), **2** (B), **3** (C), **4** (D), **5** (E), **6** (F), and **7** (G) in acetone/water (3:1) at the proton concentration of 3.8×10^{-2} M for 2, 0.25, 20, 23, 2, 22, and 1.5 h, respectively. The reaction products of **1**–**3** and **5**–**7** were eluted on a reverse-phase column 5C₁₈-AR-II (6 mm i.d. \times 250 mm) with methanol at a flow rate of 1.0 mL/min. The reaction products of **4** were eluted on a reverse-phase column 3C₁₈-EB (4.6 mm i.d. \times 150 mm) with methanol at a flow rate of 0.3 mL/min. Chromatograms A–G were recorded at 407, 404, 407, 420, 404, 411, and 404 nm, respectively.

exhibited the main products at 23 min, which were ascribable to **4'** ($\lambda_{\max} = 420$ and 693 nm), with a slight fraction at 12 min (Figure 8D). The broadening of the main fraction at 23 min would be characteristic of the free-base forms of formylated chlorins on reverse-phase columns (Nacalai Tesque, Inc.) and is not derived from the byproducts in the demetalation reaction. A slight byproduct was also detected at 11 min after demetalation of **6**, whereas the main product eluted at 23 min was **6'** ($\lambda_{\max} = 411$ and 682 nm; Figure 8F). A small fraction at 8 min might be ascribable to the residual zinc chlorin **6**. Both reaction products of 3¹-hydroxy compounds **5** and **7**, respectively, consisted of sole fractions, which were assigned to **5'** ($\lambda_{\max} = 404$ and 660 nm) and **7'** ($\lambda_{\max} = 404$ and 658 nm; Figure 8E,G). These analyses revealed that few side reactions occurred within the reaction time in which the demetalation

rate constants were estimated under the present reaction conditions.

CONCLUSION

The present analysis of the demetalation kinetics of systematically substituted zinc chlorins **1**–**7** clearly indicates that the demetalation rate constants of metallochlorins are correlated with the group electronegativities and Hammett σ constants of their peripheral substituents. Therefore, electron-withdrawing and -donating strength of the substituents on the chlorin π macrocycle provides useful information to understand the physicochemical properties of Chl demetalation quantitatively. These results will contribute to elucidation of the reaction mechanisms of in vivo and in vitro demetalation of the Chl molecules.

ASSOCIATED CONTENT

Supporting Information

¹H NMR and FAB-MS data of **1'**–**7'**. This material is available free of charge via the Internet at <http://pubs.acs.org>.

AUTHOR INFORMATION

Corresponding Author

*E-mail: saga@chem.kindai.ac.jp. Fax: +81-6-6723-2721.

Notes

The authors declare no competing financial interest.

ACKNOWLEDGMENTS

We thank Dr. Yuki Hirai, Nagahama Institute of Bio-Science and Technology, and Yasuhiro Iida, Kinki University, for their experimental assistance. This work was partially supported by a Grant-in-Aid for Scientific Research (C) (No. 23550201 to Y.S.) from the Japan Society for the Promotion of Science.

REFERENCES

- (1) Scheer, H. In *Chlorophylls and Bacteriochlorophylls: Biochemistry, Biophysics, Functions and Applications*; Grimm, B., Porra, R. J., Rüdiger, W., Scheer, H., Eds.; Springer: Dordrecht, The Netherlands, 2006; pp 1–26.
- (2) Tamiaki, H.; Kunieda, M. In *Handbook of Porphyrin Science*; Kadish, K. M., Smith, K. M., Guillard, R., Eds.; World Scientific: Singapore, 2011; Vol. 11, pp 223–290.
- (3) Wakao, N.; Yokoi, N.; Isoyama, N.; Hiraishi, A.; Shimada, K.; Kobayashi, M.; Kise, H.; Iwaki, M.; Itoh, S.; Takaichi, S.; Sakurai, Y. *Plant Cell Physiol.* **1996**, *37*, 889–893.
- (4) Kobayashi, M.; Akiyama, M.; Kise, H.; Takaichi, S.; Watanabe, T.; Shimada, K.; Iwaki, M.; Itoh, S.; Ishida, N.; Koizumi, M.; Kano, H.; Wakao, N.; Hiraishi, A. *Photomed. Photobiol.* **1998**, *20*, 75–80.
- (5) Kobayashi, M.; Akiyama, M.; Kise, H.; Watanabe, T. In *Chlorophylls and Bacteriochlorophylls: Biochemistry, Biophysics, Functions and Applications*; Grimm, B., Porra, R. J., Rüdiger, W., Scheer, H., Eds.; Springer: Dordrecht, The Netherlands, 2006; pp 55–66.
- (6) Klimov, V. V.; Klevanik, A. V.; Shuvalov, V. A.; Krasnovsky, A. A. *FEBS Lett.* **1977**, *82*, 183–186.
- (7) Klimov, V. V.; Shuvalov, V. A.; Heber, U. *Biochim. Biophys. Acta* **1985**, *809*, 345–350.
- (8) Hastings, G.; Durrant, J. R.; Barber, J.; Porter, G.; Klug, D. R. *Biochemistry* **1992**, *31*, 7638–7647.
- (9) Loll, B.; Kern, J.; Saenger, W.; Zouni, A.; Biesiadka, J. *Nature* **2005**, *438*, 1040–1044.
- (10) Deisenhofer, J.; Epp, O.; Miki, K.; Huber, R.; Michel, H. *Nature* **1985**, *318*, 618–624.
- (11) Allen, J. P.; Feher, G.; Yeates, T. O.; Komiyama, H.; Rees, D. C. *Proc. Natl. Acad. Sci. U.S.A.* **1987**, *84*, 5730–5734.

- (12) Kamiya, N.; Shen, J.-R. *Proc. Natl. Acad. Sci. U.S.A.* **2003**, *100*, 98–103.
- (13) Ferreira, K. N.; Iverson, T. M.; Maghlaoui, K.; Barber, J.; Iwata, S. *Science* **2004**, *303*, 1831–1838.
- (14) Guskov, A.; Kern, J.; Gabdulkhakov, A.; Broser, M.; Zouni, A.; Saenger, W. *Nat. Struct. Mol. Biol.* **2009**, *16*, 334–342.
- (15) Umena, Y.; Kawakami, K.; Shen, J.-R.; Kamiya, N. *Nature* **2011**, *473*, 55–60.
- (16) Benz, J.; Rudiger, W. *Z. Naturforsch.* **1981**, *36c*, 51–57.
- (17) Kräutler, B.; Matile, P. *Acc. Chem. Res.* **1999**, *32*, 35–43.
- (18) Hörtensteiner, S. *Annu. Rev. Plant Biol.* **2006**, *57*, 55–77.
- (19) Kräutler, B. *Photochem. Photobiol. Sci.* **2008**, *7*, 1114–1120.
- (20) Hörtensteiner, S.; Kräutler, B. *Biochim. Biophys. Acta* **2011**, *1807*, 977–988.
- (21) Saga, Y.; Tamiaki, H. *Chem. Biodivers.* **2012**, *9*, 1659–1683.
- (22) Mackinney, G.; Joslyn, M. A. *J. Am. Chem. Soc.* **1940**, *62*, 231–232.
- (23) Mackinney, G.; Joslyn, M. A. *J. Am. Chem. Soc.* **1941**, *63*, 2530–2531.
- (24) Schanderl, S. H.; Chichester, C. O.; Marsh, G. L. *J. Org. Chem.* **1962**, *27*, 3865–3868.
- (25) Rosoff, M.; Aron, C. *J. Phys. Chem.* **1965**, *69*, 21–24.
- (26) Berezin, B. D.; Drobysheva, A. N.; Karmanova, L. P. *Russ. J. Phys. Chem.* **1976**, *50*, 720–723.
- (27) Mazaki, H.; Watanabe, T. *Bull. Chem. Soc. Jpn.* **1988**, *61*, 2969–2970.
- (28) Mazaki, H.; Watanabe, T.; Takahashi, T.; Struck, A.; Scheer, H. *Bull. Chem. Soc. Jpn.* **1992**, *65*, 3212–3214.
- (29) Kobayashi, M.; Yamamura, M.; Akiyama, M.; Kise, H.; Inoue, K.; Hara, M.; Wakao, N.; Yahara, K.; Watanabe, T. *Anal. Sci.* **1998**, *14*, 1149–1152.
- (30) Saga, Y.; Hirai, Y.; Tamiaki, H. *FEBS Lett.* **2007**, *581*, 1847–1850.
- (31) Hirai, Y.; Tamiaki, H.; Kashimura, S.; Saga, Y. *Photochem. Photobiol.* **2009**, *85*, 1140–1146.
- (32) Hirai, Y.; Tamiaki, H.; Kashimura, S.; Saga, Y. *Photochem. Photobiol. Sci.* **2009**, *8*, 1701–1707.
- (33) Saga, Y.; Hojo, S.; Hirai, Y. *Bioorg. Med. Chem.* **2010**, *10*, 5697–5700.
- (34) Hirai, Y.; Kashimura, S.; Saga, Y. *Photochem. Photobiol.* **2011**, *87*, 302–307.
- (35) Hirai, Y.; Sasaki, S.; Tamiaki, H.; Kashimura, S.; Saga, Y. *J. Phys. Chem. B* **2011**, *115*, 3240–3244.
- (36) Saga, Y.; Miura, R.; Sadaoka, K.; Hirai, Y. *J. Phys. Chem. B* **2011**, *115*, 11757–11762.
- (37) Saga, Y.; Hirai, Y.; Sadaoka, K.; Isaji, M.; Tamiaki, H. *Photochem. Photobiol.* **2012**, in press.
- (38) Miyashita, H.; Ikemoto, H.; Kurano, N.; Adachi, K.; Chihara, M.; Miyachi, S. *Nature* **1996**, *383*, 402.
- (39) Murakami, A.; Miyashita, H.; Iseki, M.; Adachi, K.; Mimuro, M. *Science* **2004**, *303*, 1633.
- (40) Smith, K. M.; Kehres, L. *J. Am. Chem. Soc.* **1983**, *105*, 1387–1389.
- (41) Cheng, P.; Liddell, P. A.; Ma, S. X. C.; Blankenship, R. E. *Photochem. Photobiol.* **1993**, *58*, 290–295.
- (42) Tamiaki, H.; Takeuchi, S.; Tanikaga, R.; Balaban, S. T.; Holzwarth, A. R.; Schaffner, K. *Chem. Lett.* **1994**, 401–402.
- (43) Balaban, T. S.; Tamiaki, H.; Holzwarth, A. R.; Schaffner, K. *J. Phys. Chem. B* **1997**, *101*, 3424–3431.
- (44) Saga, Y.; Miyatake, T.; Tamiaki, H. *Bioorg. Med. Chem. Lett.* **2002**, *12*, 1229–1231.
- (45) Smith, K. M.; Goff, D. A.; Simpson, D. J. *J. Am. Chem. Soc.* **1985**, *107*, 4946–4954.
- (46) Tamiaki, H.; Amakawa, M.; Shimono, Y.; Tanikaga, R.; Holzwarth, A. R.; Schaffner, K. *Photochem. Photobiol.* **1996**, *63*, 92–99.
- (47) Johnson, D. G.; Svec, W. A.; Wasielewski, M. R. *Isr. J. Chem.* **1988**, *28*, 193–203.
- (48) Saga, Y.; Nakai, Y.; Tamiaki, H. *Supramol. Chem.* **2009**, *21*, 738–746.
- (49) Sasaki, S.; Mizutani, K.; Kunieda, M.; Tamiaki, H. *Tetrahedron Lett.* **2008**, *49*, 4113–4115.
- (50) Sasaki, S.; Mizutani, K.; Kunieda, M.; Tamiaki, H. *Tetrahedron* **2011**, *67*, 6065–6072.
- (51) Smith, K. M.; Bisset, G. M. F.; Bushell, M. J. *J. Org. Chem.* **1980**, *45*, 2218–2224.
- (52) Tamiaki, H.; Takeuchi, S.; Tsudzuki, S.; Miyatake, T.; Tanikaga, R. *Tetrahedron* **1998**, *54*, 6699–6718.
- (53) Saga, Y.; Otono, T. *Chem. Lett.* **2012**, *41*, 360–362.
- (54) Tamiaki, H.; Yagai, S.; Miyatake, T. *Bioorg. Med. Chem.* **1998**, *6*, 2171–2178.
- (55) Inamoto, N.; Masuda, S. *Chem. Lett.* **1982**, 1003–1006.
- (56) Hansch, C.; Leo, A.; Taft, R. W. *Chem. Rev.* **1991**, *91*, 165–195.
- (57) Giraudeau, A.; Callot, H. J.; Gross, M. *Inorg. Chem.* **1979**, *18*, 201–206.
- (58) Baker, E. W.; Storm, C. B.; McGrew, G. T.; Corwin, A. H. *Bioinorg. Chem.* **1973**, *3*, 49–60.
- (59) Orzel, L.; Fiedor, L.; Wolak, M.; Kania, A.; van Eldik, R.; Stochel, G. *Chem.—Eur. J.* **2008**, *14*, 9419–9430.
- (60) Orzel, L.; Kania, A.; Rutkowska-Zbik, D.; Susz, A.; Stochel, G.; Fiedor, L. *Inorg. Chem.* **2010**, *49*, 7362–7371.
- (61) Gerola, A. P.; Tsubone, T. M.; Santana, A.; de Oliveira, H. P. M.; Hioka, N.; Caetano, W. *J. Phys. Chem. B* **2011**, *115*, 7364–7373.
- (62) Chen, C.-Y.; Sun, E.; Fan, D.; Taniguchi, M.; McDowell, B. E.; Yang, E.; Diers, J. R.; Bocian, D. F.; Holton, D.; Lindsey, J. S. *Inorg. Chem.* **2012**, *51*, 9443–9464.